Coreless vortices in superfluid ^{3}He-A : Topological structure, nucleation, and the screening effect

Tin-Lun Ho
Department of Physics, University of Illinois at Urbana-Champaign, Urbana, Illinois 61801
(Received 13 February 1978)

Two simple relations connecting the superfluid circulation around any contour C enclosing a simply connected surface Σ and the texture in Σ are established. They are applied to discuss the topological structures and the nucleation of coreless vortices in superfluid ^{3}He-A. It is shown that the latter is a very different phenomenon from the nucleation of singular vortices. A vortex ring of finite size, or a pair of antiparallel vortex lines separated by a finite distance, can be formed continuously out of a uniform order parameter. Their activation energy is connected intimately with the stability of superflow recently discussed. It vanishes near $T = 0$ but happens to be nonzero near T_c. It is also suggested that at any temperature $T < T_c$ the absolute minimum of the free energy of ^{3}He-A in a container with a large surface circulation is given by a configuration with many coreless vortices confined in a tiny surface layer, so that in the bulk, the order parameter is a constant. This "screening effect," which affects strongly the amount of angular momentum carried by the fluid, is a special property of ^{3}He-A.

I. INTRODUCTION

The A phase of superfluid ^{3}He consists of triplet p-wave Cooper pairs which have unit orbital-angular-momentum projection along a certain direction $\hat{l}$ and zero-spin angular-momentum projection along another direction $\hat{d}$. As a result, the order parameter of ^{3}He-A is a complex 3×3 matrix[1]

$$A_{\mu i} = \Delta \hat{d}_\mu (\hat{\phi}_1 + i\hat{\phi}_2)_i \equiv \Delta \hat{d}_\mu \hat{\phi}_i, \tag{1.1}$$

where $\hat{\phi}_1$, $\hat{\phi}_2$, and $\hat{l}$ are unit vectors forming a right-handed triad. An important consequence of this form of the order parameter is that the superfluid velocity, defined as[2]

$$\vec{v}_s \equiv (\hbar/2m)\hat{\phi}_1 \cdot \vec{\nabla}\hat{\phi}_2, \tag{1.2}$$

possesses a distributed vorticity $\vec{\nabla}\times\vec{v}_s$, which is related to the field of the angular-momentum quantization axis $\hat{l}$ (i.e., the texture) by[2]

$$\vec{\nabla}\times\vec{v}_s = (\hbar/2m)\tfrac{1}{2}\epsilon_{\alpha\beta\gamma} l_\alpha \vec{\nabla} l_\beta \times \vec{\nabla} l_\gamma. \tag{1.3}$$

This relation immediately implies that the superfluid circulation ν,

$$\nu \equiv \oint_C \vec{v}_s \cdot d\vec{s}, \tag{1.4}$$

around any contour C is not necessarily quantized. In ^{4}He II, nonvanishing circulation demands singularities in the order parameter, whereas in ^{3}He-A, an arbitrary amount of circulation can be obtained by bending the texture in an appropriate way; no singularities are involved. The texture on the surface Σ enclosed by a contour C around which the circulation is ν will be referred to as a coreless ν vortex, since it produces the same circulation as a conventional singular vortex of strength ν.

The purpose of this paper is to discuss the topology and the problem of nucleation of these vortex textures, as well as their effects on the bulk superflow.

The nucleation of coreless vortices turns out to be very different from that of singular vortices. Two oppositely directed coreless vortex lines separated by a large distance (or a vortex ring of large radius) can be nucleated continuously from a uniform order parameter, in contrast to the nucleation of singular vortex pairs or rings, which can take place only in a tiny region. As pointed out recently,[3] it is the nucleation of coreless vortices near the surface of the container that would have upset the stability of a uniform superflow near T_c if there were no dipole coupling between the spin and orbital degrees of freedom. The stability of superflow in ^{3}He-A is therefore accidental, rather than a topological necessity, as in ^{4}He II.

The paper is organized as follows. In Sec. II, the relations between superfluid circulation and the texture on a simply connected surface are summarized in two statements. These relations are utilized in Sec. III to discuss the nucleation of a pair of antiparallel 4π vortices. In Sec. IV, we discuss the "screening effect" of the surface vortices. It is argued that the state of lowest free energy for ^{3}He-A in an anulus at any temperature $T < T_c$ constrained to have a large circulation at the surface should be the one filled with antiparallel vortex pair textures similar to that mentioned in Sec. III. The surface circulation is screened out completely by the vortex textures so that the order parameter is a constant in the bulk. Section V is a discussion on vortex rings. In the Appendix,

a generalized definition for the "induced area" introduced in Sec. II, together with some remarks about the vortex array in fast rotating ^{3}He-A, is given.

We only consider the case of zero external magnetic field. The spin vector $\hat{d}$ is then forced to lie parallel to $\hat{l}$ in order to minimize the dipole energy.[1] The system is then specified only by the complex vector $\hat{\phi}$, which we shall refer to as the order parameter. For the rest of the paper, $\hbar/2m$ is set equal to 1.

II. RELATIONS BETWEEN SUPERFLUID CIRCULATION AND THE TEXTURE IN A SIMPLY CONNECTED REGION

We first introduce the notions of the textural order-parameter space S_l^2 and the image loops. The former is the surface of a unit sphere representing all possible directions of the texture. The $\hat{l}$ vector at any space point $\vec{r}$ is represented by the vector $\hat{l}(\vec{r})$ in S_l^2. The image loop of a simple loop (no self-intersection) C in real space with a certain orientation is in general a multiple loop in S_l^2 with an induced orientation and is denoted as $D=\hat{l}(C)$. We shall, however, in our discussion consider the simplest case when D is also a simple loop. The general case when D is an arbitrary loop will be considered in the Appendix. The area enclosed by D, $\mu(D)$, is defined as the area on the left as one walks on the surface S_l^2 along the image loop $\hat{l}(C)$ with the induced orientation, [see Figs. 1(a) and 1(b)]. If two loops D and D' in S_l^2 are identical except for their orientations, then $\mu(D)=4\pi-\mu(D')$ [see Fig. 1(b)].

The properties of superfluid circulation around any contour C which encloses a simply connected surface Σ on which the order parameter is nonsingular are summarized as follows:

(a) The superfluid circulation around any simple contour C is given by

$$\oint_C \vec{v}_s \cdot d\vec{s} = \mu(D) + 4\pi m, \quad m = 0, \pm 1, \pm 2, \ldots . \tag{2.1}$$

(b) Let $\hat{\phi}^a$ and $\hat{\phi}^b$ be two order parameters with identical boundary textures on the space loop C. They, and hence their textures, are deformable into each other in Σ with the boundary texture on C held fixed if and only if they have identical circulation around C. [By "deformable" we mean there is a regular $\hat{\phi}^t$ defined in Σ, $0 \le t \le 1$, which satisfies $\hat{\phi}^0=\hat{\phi}^a$, $\hat{\phi}^1=\hat{\phi}^b$. "Keeping the boundary texture fixed" means the texture $\hat{l}^t$ of $\hat{\phi}^t$ satisfies $\hat{l}^t(C)=\hat{l}(C)$ for all t.]

To understand (2.1), let (u,v) be a coordinate system on the real space surface Σ, and (θ,φ) be a spherical coordinate system on S_l^2 with respect to a fixed set of axes $\hat{x},\hat{y},\hat{z}$, so that any vector $\hat{l}(\vec{r})$ can be represented as

$$\hat{l}(\vec{r}) = \cos\theta(\vec{r})\,\hat{z} + \sin\theta(\vec{r})[\cos\varphi(\vec{r})\,\hat{x} + \sin\varphi(\vec{r})\,\hat{y}]. \tag{2.2}$$

It is then trivial to show that

$$\oint_C \vec{v}_s \cdot d\vec{s} = \int\int_\Sigma \hat{l}\cdot\partial_u\hat{l}\times\partial_v\hat{l}\,du\,dv \tag{2.3}$$

$$= \int\int_\Sigma \sin\theta\,\frac{\partial(\theta,\varphi)}{\partial(u,v)}\,du\,dv. \tag{2.4}$$

The integrands of (2.3) and (2.4) are two different forms of the differential area in S_l^2 covered by a differential element $dudv$ in Σ at the point (u,v).[4] The circulation can therefore be interpreted as the *net* amount of area in S_l^2 covered by the surface Σ. The term "net amount" is emphasized because the Jacobian in (2.4) may change sign in different parts of Σ, thereby creating a cancellation of area in S_l^2. In case the map $\hat{l}(\vec{r})$ is one-one, the net area in S_l^2 covered is clearly $\mu(D)$, corresponding to the case $m=0$ in (2.1). In case $\hat{l}(\vec{r})$ is not one-one (but the image loop is still a simple one), when counting the net area covered in S_l^2, in addition to the minimal area $\mu(D)$ enclosed by the image loop $\hat{l}(C)$, we have to include the net number of times m that S_l^2 is wrapped around completely (see Fig. 2). Hence we have Eq. (2.1).[5]

Statement (a) immediately suggests a classification scheme: The possible order parameters that can be put into a surface Σ, while producing the same boundary texture $\hat{l}(C)$ can be divided into classes according to the net number of times their textures cover S_l^2.

Statement (b) simply says that with the boundary texture held fixed, only order parameters in the same class can be deformable into each other.[6,7]

When $\hat{l}(C)$ is a multiple loop, statements (a) and (b) remain true provided the definition of $\mu(D)$ is properly generalized. This will be done in the Ap-

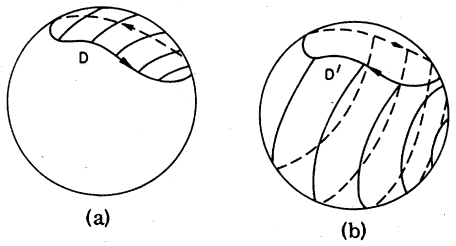

FIG. 1. Shaded areas in (a) and (b) are defined to be the areas $\mu(D)$ and $\mu(D')$ enclosed by the simple loops D and D' whose orientations are indicated by an arrow. (b) The loop D' differs from D only in orientation, hence $\mu(D')=4\pi-\mu(D)$.

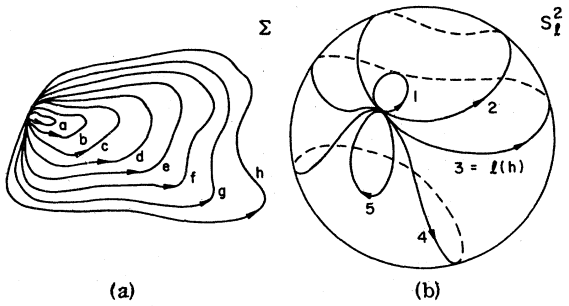

FIG. 2. Wrapping S_l^2 by a real-space surface through the map $\hat{l}(r)$: the real-space surface Σ can be considered as a collection of simple loops of identical sence [in accordance with the convention used in defining $\mu(D)$] as shown in (a). Loop h is the boundary of Σ, whose image in S_l^2 is the loop 3 in (b), i.e., $3=\hat{l}(h)$. Let us consider the following way of mapping. As the family of loops in (a) is traversed from a to h, the following sequence of loops is also traversed in S_l^2: 12345123. The total area covered in S_l^2 is therefore $4\pi+\mu(D)$, corresponding to the case $m=1$ in (2.1). If the sequence of loops in S_l^2 corresponding to $a\rightarrow h$ is $\bar{1}\bar{2}\bar{3}\bar{4}\bar{5}123$, where $\bar{1}$ is defined as loop 1 with its orientation reversed, then the net area in S_l^2 covered by Σ is $-4\pi+\mu(4)=-\mu(\bar{4})$, correspond to the case $m=-1$ in (2.1).

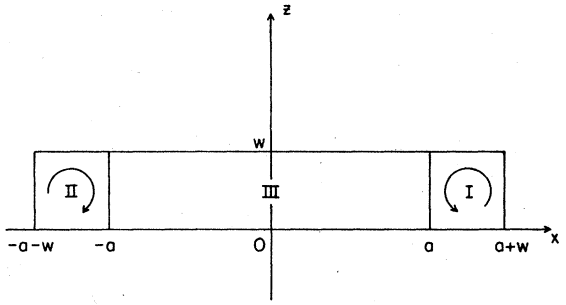

FIG. 3. Schematic representation of a pair of antiparallel vortices: the texture is uniform everywhere on the x-y plane along the z direction except in the squares I and II, which contain a $+4\pi$ and -4π vortex separately. The direction of circulation of each vortex is represented by a circular arrow.

pendix so as to complete the information contained the circulation formula (2.1). It is possible to give a rigorous proof for (a) and (b) including the general case when D is an arbitrary loop. The details of the proof will not be given here because they are lengthy. It is believed that the above remarks, together with the demonstrations in the discussions in this and the following sections, though not proofs themselves, should convince a "reasonable" person.[8]

III. FORMATION OF AN ANTIPARALLEL VORTEX PAIR

Statements (a) and (b) in Sec. II readily furnish a process for vortex formation. Let us consider only order parameters that are uniform along the y direction. We shall show below, that a state $\hat{\phi}^1$ (with texture $\hat{l}^1$) describing two isolated antiparallel vortices can be created continuously out of a state of uniform superflow and uniform texture $\vec{v}_s=u\hat{l}=u\hat{z}$, corresponding to the order parameter $\hat{\phi}^0=e^{iuz}(\hat{x}+i\hat{y})/\sqrt{2}$—a state with no vortex at all.

An example of this vortex pair texture $\hat{l}^1$ is represented schematically by Fig. 3. The two square squares labeled as I and II in Fig. 3 are the only regions in the x-z plane where $\hat{l}^1$ differs from $\hat{z}$. Both squares cover S_l^2 once but with different orientations. Therefore each of them behaves as an isolated 4π vortex. [Note that statement (a) requires that the circulation around the boundary of each square must be multiples of 4π, since the image loop in S_l^2 is just the north pole.] The entire configuration can hence be considered as a pair of vortices of opposite strength separated by a distance a. An example of $\hat{l}^1$ can be written down with the aid of (a):

$$\hat{l}^1(x,z)=R(\hat{n}(x),-\psi(z))\hat{z}, \tag{3.1}$$

where $R(\hat{n}(x),-\psi(z))$ represents a rotational matrix with rotational axis $\hat{n}$ and rotational angle $-\psi$, so that for any vector $\vec{a}$,

$$R(\hat{n},\theta)\vec{a}=(\vec{a}\cdot\vec{n})\hat{n}+\cos\theta[\vec{a}-(\vec{a}\cdot\vec{n})\hat{n}] + \sin\theta\hat{n}\times\vec{a}. \tag{3.2}$$

The rotational angle $\psi(z)$ is a monotonic and smooth function which remains 0 for $z\leq 0$ and 2π for $z\geq w$. The rotational axis $\hat{n}(x)$ is a smooth one-dimensional vector field of the form

$$\hat{n}(x)=\cos\zeta(x)\,\hat{z}+\sin\zeta(x)\,\hat{x}=R(\hat{y},\zeta)\hat{z}, \tag{3.3}$$

where $\zeta(x)$ can be one of the functions $\zeta_a(x)$ and $\zeta_b(x)$ as depicted in Figs. 4(a) and 4(b). Note that

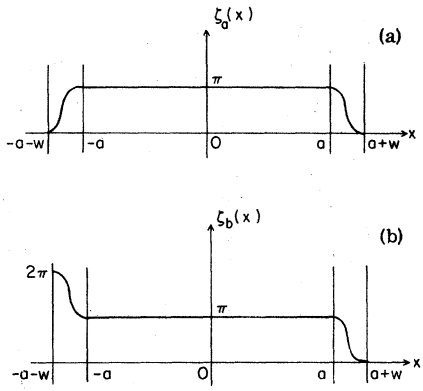

FIG. 4. Two choices for the function $\zeta(x)$ in (3.3).

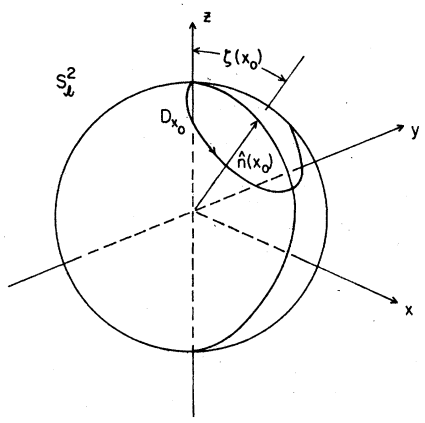

FIG. 5. Image loop D_{x_0} of the texture (3.1) generated by rotating $\hat{z}$ about $\hat{n}(x_0)$, as z decreases from w to 0 with $x=x_0$.

$\hat{n}=\hat{z}$ and $-\hat{z}$ for $|x|\geq w+a$ and $|x|\leq a$. This implies $\hat{l}^1=\hat{z}$ except in squares I and II.

To see how (3.1) describes a $\pm 4\pi$ vortex pair configuration, note that for any given x_0 between a and $a+w$, the texture $\hat{l}^1$ along the line $0\leq z\leq w$, $x=x_0$, is represented by the loop D_{x_0} in S_l^2 as shown in Fig. 5, which is generated by rotating the $\hat{z}$ axis about the rotational axis $\hat{n}$. As the angle ζ increases from 0 to π, the entire S_l^2 is covered once, giving rise to a 4π circulation around the boundary of square I. It is not difficult to see that when $\hat{n}$ is brought from $-\hat{z}$ to $\hat{z}$ through either $\zeta_a(x)$ or $\zeta_b(x)$ as x decreases from $-a$ to $-a-w$, the entire S_l^2 will be covered once but with a different orientation.

An order parameter (among many) that possesses such a vortex pair texture (3.1) is

$$\hat{\phi}^1(x,z)=e^{iuz}e^{-i\psi(z)}R(\hat{n}(x),-\psi(z))(\hat{x}+i\hat{y})/\sqrt{2}, \tag{3.4}$$

which is identical to $\hat{\phi}^0$ (the state of uniform superflow and texture $\vec{v}_s=u\hat{l}=u\hat{z}$) outside the rectangle Σ: $|x|\leq a+w$, $0\leq z\leq w$, and can therefore be regarded as a pair of antiparallel 4π vortices immersed in the middle of a uniform superflow $u\hat{z}$. It is easy[9] to work out the superfluid velocity $\vec{v}_s=\hat{\phi}_1\cdot\vec{\nabla}\hat{\phi}_2$ from (3.4),

$$\vec{v}_s=u\hat{z}-(1-\cos\zeta)\vec{\nabla}\psi-\sin\psi\sin\zeta\vec{\nabla}\zeta. \tag{3.5}$$

That the circulation around the boundaries of squares I and II in Fig. 3 is plus and minus 4π can be verified by inspection. It should be noted that in the region between the vortices (region III in Fig. 3) where $\zeta=\pi$, $\vec{v}_s$ is reduced from the uniform value u to $u-2\psi'$. Also note that this velocity field is a short-range one. It recovers to $u\hat{z}$ outside the rectangle $\Sigma=\mathrm{I}+\mathrm{II}+\mathrm{III}$, unlike the long-range dipolar field of classical vortex pairs.

On the other hand, statement (b) guarantees the deformability between the order parameters $\hat{\phi}^1$ and $\hat{\phi}^0$ inside the rectangle $\Sigma=\mathrm{I}+\mathrm{II}+\mathrm{III}$ in Fig. 3 because they have identical texture and circulation at the boundary of Σ. An example of such a deformation is

$$\hat{\phi}^t(x,z)=e^{iuz}e^{-i\psi}R(\hat{n}(x;t),-\psi)(\hat{x}+i\hat{y})/\sqrt{2}, \quad 0\leq t\leq 1 \tag{3.6}$$

where $\hat{n}(x;t)$ can be either $\hat{n}_a$ or $\hat{n}_b$ defined below, depending on whether the function $\zeta(x)$ in (3.3) is chosen as ζ_a or ζ_b,

$$\hat{n}_a(x;t)=\cos t\zeta_a\hat{z}+\sin t\zeta_a\hat{x}=R(\hat{y},t\zeta_a)z, \tag{3.7}$$

$$\hat{n}_b(x;t)=R(\hat{m}(t),\zeta_b)\hat{z},$$

$$\hat{m}(t)=\cos(\tfrac{1}{2}t\pi)\hat{z}+\sin(\tfrac{1}{2}t\pi)\hat{y}. \tag{3.8}$$

As t varies from 0 to 1, (3.6) takes $\hat{\phi}^0$ continuously into $\hat{\phi}^1$ with the texture along the boundary of Σ held fixed along $+\hat{z}$ direction. Thus we have demonstrated statements (a) and (b) for the case when $\hat{l}(C)$ is a point in S_l^2.

The probability of nucleation of the vortex pair (3.4), however, is determined by the Boltzmann factor $\exp(-E_a/k_BT)$, where the activation energy E_a is the maximum of the energy difference between $\hat{\phi}^t$ and $\hat{\phi}^0$. When E_a vanishes, the bulk superflow will be unstable against the vortex nucleation. Since it is known that we bulk superflow is stable near T_c because of the nuclear dipole energy but is unstable near $T=0$,[3] absence of activation energy is ruled out in the Ginzburg-Landau region but remains possible near $T=0$. Although instability of superflow near $T=0$ does not necessarily imply spontaneous nucleation (full development) of isolated 4π vortices, it turns out to be the case for the nucleation process (3.6) with the choice $\hat{n}=\hat{n}_a$. We shall verify this remark, as well as the existence of an energy barrier near T_c, in the following analysis of the energetics of the process (3.6), whose superfluid velocity and texture, because of the choice $\hat{n}=\hat{n}_a$, assume the forms[10]

$$\vec{v}_s(t)=u\hat{z}-(1-\cos t\zeta_a)\vec{\nabla}\psi-t\sin\psi\sin t\zeta_a\vec{\nabla}\zeta_a, \tag{3.9}$$

$$\hat{l}(t)=(\cos\psi\sin^2 t\zeta_a+\cos^2 t\zeta_a)\hat{z}+\sin\psi\sin t\zeta_a\hat{y}+(1-\cos\psi)\cos t\zeta_a\sin t\zeta_a\hat{x}. \tag{3.10}$$

Let us recall the expressions of the free-energy density f and the mass current $\vec{g}$ of ^{3}He-A.[11]

$$f(\vec{v}_s,\hat{l})=\tfrac{1}{2}\rho_s v_s^2-\tfrac{1}{2}\rho_0(\vec{v}_s\cdot\hat{l})^2+c\vec{v}_s\cdot\vec{\nabla}\times\hat{l}-c_0(\vec{v}_s\cdot\hat{l})(\hat{l}\cdot\vec{\nabla}\times\hat{l})+\tfrac{1}{2}K_s(\vec{\nabla}\cdot\hat{l})^2+\tfrac{1}{2}K_t(\hat{l}\cdot\vec{\nabla}\times\hat{l})^2+\tfrac{1}{2}K_b(\hat{l}\times\vec{\nabla}\times\hat{l})^2, \tag{3.11}$$

$$\vec{g}(\vec{v}_s,\hat{l})=\rho_s\vec{v}_s-\rho_0(\vec{v}_s\cdot\hat{l})\hat{l}+c\vec{\nabla}\times\hat{l} - c_0(\hat{l}\cdot\vec{\nabla}\times\hat{l})\hat{l}. \quad (3.12)$$

When both $\hat{l}$ and $\vec{v}_s$ are uniform, the anisotropy ρ_0 of the superfluid density favors alignment of $\vec{v}_s$ and $\hat{l}$—a choice that has already been made in (3.4) and $\hat{\phi}^0$. Writing (3.6) as $\hat{\phi}^t=e^{iuz\hat{\epsilon}^t}$, the energy difference between $\hat{\phi}^t$ and $\hat{\phi}^0$ can be cast into the form

$$\delta F(t)=F(\hat{\phi}^t)-F(\hat{\phi}^0) =\int f(\vec{v}\cdot\hat{l})+\vec{u}\cdot\int\vec{g}(\vec{v},\hat{l})+\tfrac{1}{2}\rho_0u^2\int[1-(\hat{l}\cdot\hat{z})^2], \quad (3.13)$$

where $\vec{v}$ and $\hat{l}$ are the superfluid velocity and texture associated with $\hat{\epsilon}^t$, the vortex pair structure in the rest frame of the background superfluid $u\hat{z}$. The quantities $f(\vec{v},\hat{l})$ and $\vec{g}(\vec{v},\hat{l})$ are the energy and mass-current densities of the order parameter $\hat{\epsilon}^t(x,z)$.

Let us first consider region III in Fig. 3, where $\zeta_a=\pi$, and $\hat{\epsilon}^t$ (hence $\vec{v}$ and $\hat{l}$) depends on z only. Since $\psi^1\sim\vec{\nabla}l\sim1/w$, the energy change in region III must be of the form

$$\delta F_{\rm III}(t)=au[\mathfrak{A}(t)K(1/wu)+\mathfrak{B}(t)\rho_s+\mathfrak{C}(t)\rho_0wu], \quad (3.14)$$

where $\mathfrak{A},\mathfrak{B},\mathfrak{C}$ are bounded functions of t only, and K is the largest of the bending coefficients at that temperature. In particular, $\mathfrak{A}$ and $\mathfrak{C}$ must be positive since the first and the third terms in (3.9) are positive. The function $\mathfrak{B}(t)$ can be evaluated exactly, and is always negative as long as the result of microscopic theory[11] $\rho_s^{\parallel}\equiv\rho_s-\rho_0=c_0$ for all temperatures $T<T_c$ is adopted

$$\mathfrak{B}(t)=-\pi(1-\mu)\{2(\rho_s^{\parallel}-c_0)+\rho_0(1+3\mu^2)(1-\mu^2) +c_0[(1+\mu^3)^2+(1-\mu+\mu^4)\times(1-\mu^2)+2\mu^4]\},$$

where $\mu=\cos(t\pi)$. Note that the energy change $\delta F_{\rm III}(t)$ will be negative when the term $\mathfrak{B}(t)$ in (3.14), arising from the reduction of current $\vec{g}(\vec{v},\hat{l})=\vec{g}(\hat{\phi}^t)-\vec{g}(\hat{\phi}^0)$, outweighs the bending energy $\mathfrak{A}(t)$ and the additional kinetic energy $\mathfrak{C}(t)$ due to the anisotropy of the superfluid density. This is indeed the case near $T=0$, where microscopic theory predicts that ρ_0 vanishes as some power of T, and K diverges as $\ln T$.[11] Neglecting ρ_0 in (3.14), a t-dependent width $w=w(t)$ satisfying $wu\rho_s\mathfrak{B}(t)=-2\mathfrak{A}(t)K$ renders $\delta F_{\rm III}(t)$ negative. Yet, the energy reduction in region III can be enormously amplified by increasing the vortex separation a, so much so that the energy changes in regions I and II are no longer significant, since they are independent of a and must be a bounded function. The total energy change $\delta F(t)$ then is given essentially by $\frac{1}{2}\mathfrak{B}(t)\rho_s(ua)<0$. Near $T=0,(\rho_0\sim0)$, it is easy to show that $\partial\mathfrak{B}/\partial t<0$ for all $0\leq t\leq1$. Spontaneous vortex nucleation hence follows.

Of course, if spontaneous nucleation were possible, there would be no reason to have just one vortex pair. Rather, one would expect simultaneous nucleation of many pairs, creating a structure filled with vortex pair textures. We shall come to this in Sec. IV. The above calculation also implies that for all $T<T_c$, once a $\pm4\pi$ vortex pair is formed (in general, an energy barrier must be overcome in order to achieve this), so that $\mathfrak{C}(1)=0$ in region III in Fig. 3, the vortex pair configuration will be of lower energy than the original one ($\vec{v}_s\parallel\hat{l}$) and will start expanding, provided the vortex size w and the separation a exceed certain critical values, say, $w_{\rm cr}=-2\mathfrak{A}(1)K/\mathfrak{B}(1)\rho_s$ and $a_{\rm cr}=[-\delta F_{\rm I+II}(1)/\frac{1}{2}\mathfrak{B}(1)\rho_s]u$. Both $a_{\rm cr}$ and $w_{\rm cr}$ are of the order of $1/u$, or more precisely, $\hbar/2mu$.[12]

Near T_c, dipolar coupling between the texture and the spin axis $\hat{d}$ implies $K_s=K_t=K_b=K$.[11] It can be shown that for small t, (3.13) becomes

$$\delta F(t)=\int dz\,dx\,2\left(\sin\frac{\psi}{2}\right)^2\left[K\left(\frac{\psi'}{2}-\frac{u}{K}\left(\tfrac{1}{2}\rho_s''+c_0\right)\right)^2+K\left(\frac{\psi'}{2}\cot\frac{\psi}{2}\right)^2+\rho_0u^2\left(1-\frac{1}{\rho_0K}\left(\tfrac{1}{2}\rho_s^{\parallel}+c_0\right)\right)\right](\xi t)^2$$

which is positive because the ratio $(\frac{1}{2}\rho_s^{\parallel}+c_0)/\rho_0K$ is less than one.[3] Hence an energy barrier exists for the path (3.6) near T_c. Whether the temperature at which the activation energy ceases to be negative or becomes comparable to k_BT lies above the A-B transition is rather difficult to estimate.

IV. SCREENING EFFECT OF SURFACE VORTICES IN CONTAINERS WITH LARGE SURFACE CIRCULATIONS

Consider ^{3}He-A in an annulus made up of two concentric cylinders of radius R and $R+a$, (toroidal container will be considered in Sec. V). Close to the surface, the texture is normal to

the wall due to boundary depairing effects.[13] The order parameter space on the surface is therefore reduced down to a circle—the angle between $\hat{\phi}_1$ and the tangent of the surface contour. Circulation is quantized in units of 2π around both inner and outer boundaries.[14] In this section, we will discuss the state of lowest free energy of ^{3}He-A *at any temperature* $T < T_c$ in an annulus when the circulation N on both surface are identical and large, $N \gg R/a$.[15] What the inequality means is that if the $2\pi N$ circulation on the surface is due to a superfluid velocity of the form $(N/r)\hat{\varphi} \equiv u(R/r)\hat{\varphi}$ circulating around the annulus, (r and φ being cylindrical coordinates), the critical size $1/u$ of a vortex pair allowed by this superflow (see the second last paragraph in Sec. III) must be smaller than the dimension of the container a.

One might imagine that a stationary point of the free energy would be a configuration consisting of this large, circulating superflow $\vec{v}_s = u(R/r)\hat{\varphi}$ with $uR = N$, and a texture aligned with it inside the annulus except in a surface layer of thickness D, where $\hat{l}$ must turn perpendicular to the wall. We denote this configuration as $\hat{\Phi}_i$. If the texture of $\hat{\Phi}_i$ lies in the x-y plane, in the limit of large R, and the condition $u \gg 1/a$ is maintained, then $\hat{\Phi}_i$ reduces to the de Genne–Rainer configuration for the parallel-plate geometry in the strong-flow limit.[16] It is easy to show that the thickness D of the vortex layer is roughly $1/u$. The energy of the system is of the order of $\frac{1}{2}\rho_s u^2(2\pi Ra)$—a consequence of the almost uniform velocity profile and the tiny surface layers.

It has been pointed out[17] that this state is not stationary because its surface layers are unstable. Even if it could be shown that a readjustment of the texture near the surface were enough to eliminate this instability, $\hat{\Phi}_i$ is by no means the absolute minimum. We simply observe that because of the condition $u \gg 1/a$, replacement of certain amount of uniform texture in the bulk by a vortex pair texture (3.4) of sufficiently large size already lowers the energy.

In fact, we believe that the state of lowest free energy $\hat{\Phi}_f$, at any temperature $T < T_c$, must contain $\pm 4\pi$ vortex pairs as shown in Fig. 6. It consists of a layer of $+4\pi$ and a layer of -4π vortices attached to the outer and inner surfaces. This can be viewed alternatively as a series of rectangular cells, each contains a $\pm 4\pi$-vortex pair configuration of the form (3.4) in Sec. II. Each 4π vortex is confined in a rectangle of size $s \times w$. The region sandwiched between the vortex layers (between the contours C_1 and C_2 in Fig. 6) has zero superfluid velocity and a uniform (or extremely slowly varying) texture. The energy in this region is essentially zero. The total number of 4π vortices in

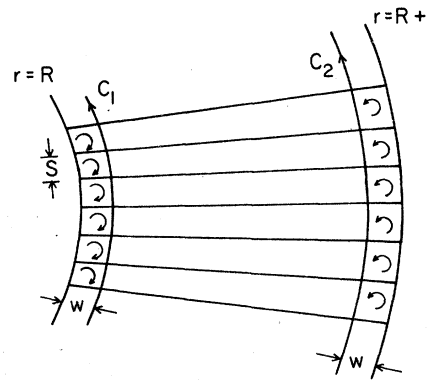

FIG. 6. Schematic representation of the state of minimum free energy in an annulus with a large number of surface circulation. Roughly speaking, it is made up of a series of rectangular cells, each contains a pair of antiparallel vortices. The clockwise and counterclockwise arrows represent a $+4\pi$ and a -4π vortex separately. The superfluid velocity is zero in the region between the contours C_1 and C_2. The texture in this region is uniform.

each layer is clearly $N/2$,[18] in order to reduce the circulation at the surface down to zero at C_1 and C_2. The width s is therefore given by $s = 2\pi R/\frac{1}{2}N = 4\pi/u$. To estimate the thickness w, note that the energy of $\hat{\Phi}_f$ is contained in the vortex layers. The fact that $\vec{v}_s$ drops to zero from u within each layer implies that the kinetic energy is of the order of $\frac{1}{2}\rho_s u^2 w(2\pi R)$, while the bending energy of the texture is given by $\frac{1}{2}K(1/w)^2 w(2\pi R) \sim \frac{1}{2}K(2\pi R)/w$. The sum of these two contributions is a minimum when $w \sim 1/u$. The energy of $\hat{\Phi}_f$ is therfore roughly $\frac{1}{2}\rho_s u^2 w(2\pi R)$, which when compared with that of $\hat{\Phi}_i$, is a factor $w/a = 1/ua$ smaller. This is also the ratio of the angular momenta L_f and L_i carried by $\hat{\Phi}_f$ and $\hat{\Phi}_i$, i.e., $L_f/L_i = w/a$. This difference in angular momentum is due to the fact that the surface vortices in $\hat{\Phi}_f$ succeeded in reducing the bulk mass current, which would have other wise contributed to the total angular momentum, completely down to zero.

We can see from the above discussions that regardless of the shape of the container (cylinders, torus, etc.), as long as the surface circulation is large, the state of lowest free energy will consist of a layer of surface vortices "screening" out the surface circulation, so that the order parameter is a constant in the bulk. It should also be noted that although a layer of *singular* vortices near the surface can similarly eliminate the bulk superflow (without formation of vortex textures), such a configuration is unstable. The singular vortex layer will simply move toward the surface and annihilate the entire surface circulation after meeting its

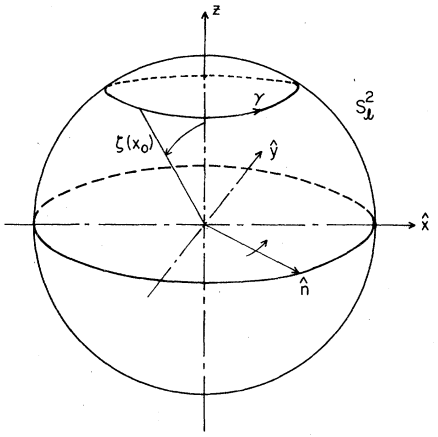

FIG. 7. Texture of (4.2) is of the form $\hat{l}(x,z) = R(\hat{n}(z), \zeta_a(x)t)\hat{z}, \hat{n} = R(\hat{z}, -uz/2)\hat{y}$. At any t, as z decreases from $w = 4\pi/u$ to 0, with $x = x_0$, the loop γ is traced out in S_l^2.

death there.[19] The existence of surface vortices and their screening effect (reminding one of Meissner effect in superconductivity) are unique properties of ^{3}He-A.

To write down an explicit example for $\hat{\Phi}_i$ and $\hat{\Phi}_f$ in an annulus, let us simulate the annulus by a pair of parallel plates located at $x = \pm(a+w)$ normal to the x axis ($a \gg w, w \sim 1/u$), with periodic boundary condition $\hat{\Phi}(x,z) = \hat{\Phi}(x, z+2\pi R)$ imposed on the order parameter. The states $\hat{\Phi}_i$ and $\hat{\Phi}_f$ are just end points of continuous family, [cf. Eq. (3.6)],

$$\hat{\Phi}(x,z;t) = e^{iuz/2} R(\hat{y},\eta) R(\hat{n}_a(x;t), -uz/2) \times (\hat{x}+i\hat{y})/\sqrt{2}, \quad 0 \le t \le 1, \tag{4.1}$$

where $\hat{n}_a$ is the vector defined in (3.7) which changes from $\hat{z}$ to $-\hat{z}$ in the bulk region $|x| \le a$ as t varies from 0 to 1. The function $\eta(x)$ differs from 0 only within a surface layer of thickness $w \sim 1/u$ from the surfaces $x = \pm(a+w)$, where it grows from 0 to $\pi/2$ (or $-\pi/2$) to satisfy the surface boundary condition.[13] Quantization of circulation at the surfaces of the annulus is still $uR = N$. In the bulk region $|x| \le a$, as t varies from 0 to 1, (4.1) changes continuously from the uniform flow configuration $e^{iuz}(\hat{x}+i\hat{y})/\sqrt{2}$ to the constant $(\hat{x}+i\hat{y})/\sqrt{2}$. Note that smooth function $\psi(z)$ in (3.4) has been changed to $uz/2$ so that $\hat{\Phi}(x,z;t)$ has a periodicity $4\pi/u$ along the z direction to characterize a vortex array.

The family (4.1) demonstrates the topological equivalence between $\hat{\Phi}_i$ and $\hat{\Phi}_f$ in an annulus explicitly.[20] Furthermore, the calculation in Sec. III indicates that $\hat{\Phi}_i$ will decay into $\hat{\Phi}_f$ spontaneously near $T = 0$, though not near T_c.[21]

Although the stability of bulk superflow near T_c reduces the likelihood of appearance of the vortex array $\hat{\Phi}_f$, it does not eliminate the possibility entirely; unless it can be shown that in the course of building up the surface circulation, a bulk superflow must result. Close to T_c, if dipole energy were neglected, it was shown in Ref. 3 that a vortex array similar to (4.1) would appear. Some of its features, however, are quite different from that of (4.1), which we shall mention below, (a point we shall also come to in Sec. V).

Again we simulate the annulus by a pair of parallel plates as in (4.1). The nucleation process that would have occurred near T_c is[22]

$$\hat{\Psi}(x,z;t) = e^{iuz} R(\hat{y},\eta) R(R(\hat{z}, -uz/2)\hat{y}, t\zeta_a(x)) \times (\hat{x}+i\hat{y})/\sqrt{2}, \quad 0 \le t \le 1, \tag{4.2}$$

where $\zeta_a(x)$ is the function in Fig. 4(a), and $R(\hat{y},\eta)$ is the same rotation that appeared in (4.1). In the bulk region, $|x| \le a$, where $\eta = 0, \zeta_a = \pi$, (4.2) is just Eq. (9) of Ref. 3 with $b = \frac{1}{2}$. At any t between 0 and 1, (4.2) corresponds to an array of $\pm\nu(t)$-vortex pairs, $\nu(t) = 2\pi(1 - \cos\pi t)$. To see that, let us first forget about the rotation $R(\hat{y},\eta)$, which only changes the texture near the surface and has no effects on $\vec{v}_s$ away from the surface layer. For any x_0 between a and $a+w$, the texture of (4.2) along the line $(0 \le z \le 4\pi/u, x = x_0)$ is just the circle γ in S_l^2 as shown in Fig. 7. As $\zeta_a(x)$ increases from 0 to π (or x decreases from $a+w$ to a), an area $\nu(t)$ is covered in S_l^2 by the rectangle $(a \le x \le a+w, 0 \le z \le 4\pi/u)$, which can then be regarded as a vortex of strength $\nu(t)$.

The difference between (4.1) and (4.2) is that the texture of $\hat{\Psi}(t=1)$ is not uniform along the boundary of the rectangular cell $|x| \le a+w, 0 \le z \le 4\pi/u$ [again, let us forget about the rotation $R(\hat{y},\eta)$]. For example, $\hat{l}$ changes from $-\hat{z}$ to $\hat{z}$ along the top (or the bottom) of the cell as $|x|$ increases from 0 to $a+w$. Hence, a single cell of $\hat{\Psi}(t=1)$ cannot appear in a uniform flow, in contrary to (3.4). Its nucleation in an annulus is made possible by the periodic boundary condition.

V. VORTEX RINGS

Any order parameter that produces a toroidal superfluid velocity field can be regarded as a vortex ring. In this section, we would like to point out that the so-called particlelike solitons[23] (which will be defined immediately) are in fact topologically equivalent to vortex rings—that is, they can be deformed into structures that produce a toroidal velocity field. Particlelike solitons are defined as those regular order parameters that can be fit into a volume Ω, subject to the boundary condition that they must reduce to a constant $\hat{\Phi}^0$ at the surface of Ω. It was pointed out by Volovik and

Mineev[23] that these solitons are characterized by an interger J,

$$J=\left(\frac{1}{4\pi}\right)^2\int \vec{v}_s\cdot\vec{\nabla}\times\vec{v}_s\,d^3x; \tag{5.1}$$

and only solitons with the same J are deformable into each other, with the order parameters at the surface held fixed at $\hat{\Phi}^0$. The interger J essentially records the number of times the order parameter space P_3 (definition given in Ref. 7) is wrapped around by the space volume Ω.

Without loss of generality, Ω can be taken as a cylinder: $0\leq r\leq a+w$, $0\leq z\leq w$, $0\leq\varphi\leq 2\pi$, where r, z, φ are cylinder coordinates. To establish the topological equivalence between a J soliton and a vortex ring, we shall write down explicitly, for each J, the expression of a J soliton which also has a toroidal velocity field. Example of these J solitons are:

$$\Phi_J(r,\varphi,z)=e^{-i\psi(z)}R(\hat{n}_J(r,\varphi),-\psi(z))(\hat{x}+i\hat{y})/\sqrt{2}, \tag{5.2}$$

$$\hat{n}_J(r,\varphi)=R(\hat{m}_J,\zeta(r))\hat{z}, \tag{5.3}$$

$$\hat{m}_J(r,\varphi)=R(\hat{z},-J\varphi)\hat{y}, \tag{5.4}$$

where $\psi(z)$ is the same function ψ appeared in (3.1), while $\zeta(r)$ is identified with the $x>0$ branch of the function $\zeta(x)$ in (3.3). The superfluid velocity of $\hat{\Phi}_J$ is of the form

$$\vec{v}_s^J=-(1-\cos\zeta)\vec{\nabla}\psi-\sin\psi\sin\zeta\vec{\nabla}\zeta +J\sin^2\zeta(1-\cos\psi)\vec{\nabla}\varphi. \tag{5.5}$$

Since $\zeta(r=a+w)=0$ (hence $\hat{n}_J=\hat{z}$) for all φ, and $\psi(z=0)=\psi(z=w)-2\pi=0$, for all r and φ, $\hat{\Phi}_J$ clearly reduces to the constant $(\hat{x}+i\hat{y})/\sqrt{2}$ at the surface of the cylinder Ω. That (5.2) is indeed a J soliton can be verified by evaluating the integral (5.1) with $\vec{v}_s=\vec{v}_s^J$.

The toroidal character of the velocity field $\vec{v}_s^J$ can be observed from (5.5) by inspection. If one is not satisfied with that, consider the texture $\hat{l}^J$ of (5.2). The first formula given in Ref. 9 enable us to rewrite $\hat{l}^J$ as

$$\hat{l}^J(r,\varphi,z)=R(\hat{z},-J\varphi)R[R(\hat{y},\zeta(r))\hat{z},-\psi(z)]\hat{z}, \tag{5.6}$$

which can be considered as obtained from texture (3.1) by rotating its $x>0$ branch through an angle $-J\varphi$ about the $\hat{z}$ axis. As we have seen in Sec. III, in the half plane $x>0$, texture (3.1) equals to $\hat{z}$ everywhere except in the square I in Fig. 5, where it covers S_I^2 once and thereby creating a 4π circulation around the boundary of square I. As a result, the vortex ring texture (5.6) is just a textural distortion confined to the ring $a\leq r\leq a+w$, $0\leq z\leq w$, $0\leq\varphi\leq 2\pi$, but is otherwise equal to $\hat{z}$ everywhere. Any plane that passes through the z axis will reveal a cross section of the ring, which also looks like Fig. 5—i.e., it contains a pair of $\pm 4\pi$ vortices. [For example, the textural cross sections of $\hat{\Phi}_{J=0}$ and $\hat{\Phi}_{J=-1}$ in the x-z plane are just the texture (3.1) with $\zeta=\zeta_a$ and $\zeta=\zeta_b$.] The toroidal character of the velocity field now becomes evident.

Note that $\hat{\Phi}_{J=0}$ is equivalent to the constant $(\hat{x}+i\hat{y})/\sqrt{2}$, which obviously has $J=0$. This can be seen by replacing the function $\zeta(r)$ in $\hat{\Phi}_{J=0}$ by $t\zeta(r)$, $0\leq t\leq 1$. The resulting family takes $\hat{\Phi}_{J=0}$ continuously into $(\hat{x}+i\hat{y})/\sqrt{2}$. Furthermore, the analysis in Sec. III implies that formation of a large $\hat{\Phi}_{J=0}$ ring is spontaneous near $T=0$ in a uniform flow. Nucleation of a $J\neq 0$ ring, on the contrary, will generate singularities.

However, vortex rings are not necessarily particlelike solitons. For example, the deformation (4.2) that would have occurred near T_c in the absence of dipole locking, when generalized to the case of a torus, becomes an array of vortex rings, each confined in a cylindrical box of height $4\pi/u$. To see this, we simply replace the rotation $R(\hat{y},\eta(x))$ and the function $\zeta_a(x)$ in (4.2) by $R(\hat{\varphi},\eta(r))$ and $\zeta(r)$, where the functions $\eta(r)$, and $\zeta(r)$ are identified with the $x>0$ branch of $\eta(x)$ and $\zeta_a(x)$. However, we mentioned in the last section that a single "box" of this order parameter cannot exist in a uniform flow [even without the rotation $R(\hat{\varphi},\eta(r))$] because of the mismatch of boundary textures, in contrast to the isolated vortex rings. Nevertheless, it has a toroidal superfluid velocity field. A fact that justifies the nomenclature and can be verified by simple calculation

$$\vec{v}_s=(1+\cos t\zeta)\vec{\nabla}\left(\frac{uz}{2}\right)+\sin t\zeta\sin\left(\frac{uz}{2}+\varphi\right)\vec{\nabla}\eta +\left[(1-\cos\eta)\cos t\zeta-\sin\eta\cos\left(\frac{uz}{2}+\varphi\right)\sin t\zeta\right]\vec{\nabla}\varphi. \tag{5.7}$$

ACKNOWLEDGMENTS

I would like to thank N. D. Mermin for constantly challenging discussions which have been inspiring and educating. Most of this work is based on part of a Ph.D thesis submitted to Cornell University, which was supported by the Material Science Center of Cornell University. The entire work was completed at Nordita through the generous support of the Physics Department of University of Illinois at Urbana-Champaign. Research supported in part by NSF Grant No. DMR 76-24011 at the University of Illinois and NSF Grant No. DMR 74-23494 at Cornell University.

APPENDIX: GENERALIZATION OF THE DEFINITION OF THE INDUCED AREA $\mu(D)$

We consider the general case when $D=\mu(C)$ is an arbitrary loop. The space loop C remains simple. We shall show that any complicated loop in S_l^2 can be decomposed into a collection of simple loops Λ_i with multiplicity λ_i, and we write $D=\sum_i \lambda_i \Lambda_i$. That is to say, as the space loop C is followed once with a fixed orientation in real space, the simple loops Λ_i in S_l^2 are covered λ_i times with their induced orientations. Two simple loops that differ only by orientations are considered distinct. The induced area of D is then defined as $\mu(D)=\sum_i \lambda_i \mu(\Lambda_i)$.

To see such a decomposition is possible, it is sufficient to show that any loop D in S_l^2 contains at least one simple loop. Let us pick a vertex (the intersection point of two lines) P_0. Then, we follow a line segment going away from this vertex. (There may be more than one such line segments.) After hitting another vertex P_1, we follow another line segment that leaves P_1, so on and so forth. Since there are finite number of vertices, eventually we will come back to P_0. If we list the vertices in their order of appearances as we go out from P_0 in the above fashion, $P_0P_1P_2,\ldots,P_NP_0$, the existence of a simple loop is evident. The reason is that there must be a cycle $P_iP_{i+1},\ldots,P_{i+m}$ in the above sequence of vertices such that $P_i=P_{i+m}$ and all P_{i+k} are distinct for $1\leq k\leq m$. Such a cycle is nothing but a simple loop. (Also see Fig. 8.)

With this generalization, statement (a) in Sec. II immediately implies that circulation must be quantized in units of 4π around the boundary C of any unit cell in the periodic texture contained in a rotating container. To see this, let us label the vertices of a unit cell in the counterclockwise direction as P_0, P_1, P_2, and P_3. We can then write $C=\sum_{i=0} P_iP_{i+1}$ with $P_4\equiv P_0$, and $\hat{l}(C)=\sum_{i=0}^{3}\gamma_i$ with $\gamma_i\equiv\hat{l}(P_iP_{i+1})$. Since all $\hat{l}(P_i)$ are identical, γ_i must be a closed loop. In particular γ_0 and γ_2 (also γ_1 and γ_3) must be identical but oppositely oriented loops. This implies the sum $\mu(\gamma_0)+\mu(\gamma_2)$ is a multiple of 4π. The conclusion that $\mu(\hat{l}(C))=4\pi m$ (m integer) hence follows.

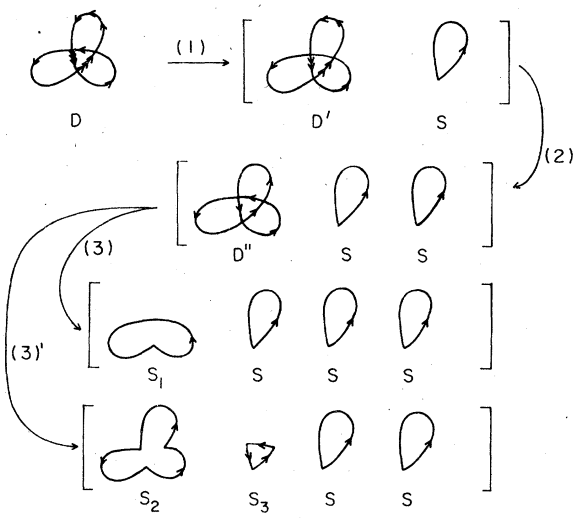

FIG. 8. Decomposition of an image loop D into simple loops. The number of arrows on each line segment between two intersection points represents the multiplicity of that line segment. After three decompositions (1)→(2)→(3), D is reduced to four simple loops $S_1+S+S+S$. The decomposition is, however, not unique. The decomposition (1)→(2)→(3)′ reduces D to the simple loops S_2+S_3+S+S. It is not difficult to convince oneself that the area $\mu(D)$, defined as $\sum_i \lambda_i \mu(\Lambda_i)$, is independent of the decomposition.

---

[1] For a general survey of ^{3}He-A, see A. J. Leggett, Rev. Mod. Phys. 47, 331 (1975); also see P. W. Anderson and W. F. Brinkman, in *The Helium Liquids*, edited by J. G. M. Armitage and I. E. Farquhar (Academic, New York, 1975).

[2] N. D. Mermin and Tin-Lun Ho, Phys. Rev. Lett. 36, 594 (1976).

[3] P. Bhattacharyya, T-L Ho, and N. D. Mermin, Phys. Rev. Lett. 39, 1290, 1691 (1977).

[4] The line segments on S_l^2 generated by the changes du (fixed v) and dv (fixed u) are $\partial_u\hat{l}\,du$ and $\partial_v\hat{l}\,dv$. Since their cross product is parallel to $\hat{l}$, the magnitude of the induced area $|\partial_u\hat{l}\times\partial_v\hat{l}|\,dudv$ is just $\pm\hat{l}\cdot\partial_u\hat{l}\times\partial_v\hat{l}\,dudv$.

[5] The circulation formula (2.1) with $\mu(D)=0$ for the special case when $\hat{l}(C)$ is a single point in S_l^2 has been considered by S. Blaha [Phys. Rev. Lett. 36, 874 (1976)] and G. Volovik and N. Kopnin {Pis'ma Zh. Eksp. Teor. Fiz. 25, 26 (1977) [JETP Lett. 25, 22 (1977)]}.

[6] It is obvious that order parameters in different classes are not deformable into each other. Since the superfluid circulation is a continuous function of the texture [see Eq. (2.3)], textures in different classes (hence their corresponding order parameters) cannot be topologically equivalent. The converse, i.e., that order parameters with identical texture and circulation at the boundary are deformable into each other, is not as obvious. The proof will not be given here because of its length and can be found in Tin-Lun Ho, Ph.D. thesis (Cornell University, unpublished). Also see Ref. 7.

[7] In the language of homotopy theory, which is currently used to classify singular and nonsingular structures of broken symmetries, [see, for example, G. Toulouse and K. Kleman, J. Phys. Lett. (Paris) 37, 149 (1976); also G. E. Volovik and V. Mineev, Zh. Eksp. Teor. Fiz. 73, 767 (1977) [Sov. Phys.-JETP (to be published)]}, the classification here corresponds to asking what are the

topologically equivalent classes of mappings that take a square into P_3 with boundary of the square mapped into a subspace A of P_3, where P_3 is of the order parameter space of $\hat{\phi}$, which is the set of all possible rotations that act on $(\hat{x}+i\hat{y})/\sqrt{2}$. In our case, A is just a fixed (trivial) loop in P_3, or equivalently, a circle S_1. The collection of such classes is called the relative homotopy group $\pi_2(P_3, S_1)$, which can be computed through the homotopy exact sequence $\pi_2(P_3) \to \pi_2(P_3, S_1) \to \pi_1(S_1) \to \pi_1(P_3)$, or $0 \to ? \to Z \to Z_2$, and is determined as the set of even integers [which turns out to be twice the integer m in Eq. (2.1)]. For the mathematical aspect of relative homotopy group, see, P. J. Hilton, *An Introduction to Homotopy Theory*, (Cambridge U. P., Cambridge, England, 1953), p. 16 and pp. 34–37.

[8]See Tin-Lun Ho in Ref. 6. The standard of "reasonableness" is suggested by M. Kac's remark "A demonstration convinces a reasonable man, a proof, a stubborn one." [Reference 2 of N. D. Mermin, Phys. Rev. 171, 272 (1968).]

[9]The relations $R(R_1\hat{n}, \theta) = R_1 R(\hat{n}, \theta) R_1^{-1}$, $\delta R(\hat{n}, \theta)\vec{a} = R(\hat{n}, \theta)(\hat{n} \times \vec{a})\delta\theta + R\delta\vec{a}$, when $\delta\hat{n} = 0$, $R(\vec{a} \times \vec{b}) = R\vec{a} \times R\vec{b}$, and $R\vec{a} \cdot R\vec{b} = \vec{a} \cdot \vec{b}$ ease things a great deal.

[10]The path (3.6) does not satisfy $\vec{\nabla} \cdot \vec{g} = 0$, where $\vec{g}$ is the mass current. This, however, presents no difficulties. It simply means that a lower energy path satisfying $\vec{\nabla} \cdot \vec{g} = 0$ exists. Such a path can be obtained by augmenting the original $\vec{v}_s$ by a potential flow $\vec{\nabla}\theta$ (with $\hat{l}$ unchanged) so that the resulting current $\vec{g}'$, which is related to the original current $\vec{g}$ by $\vec{g}' = \vec{g} + \vec{\rho}_s \cdot \vec{\nabla}\theta$, satisfies $\vec{\nabla} \cdot \vec{g}' = 0$. It can be shown that the change in free energy due to such a shift in $\vec{v}_s$ is $-\frac{1}{2}\int \vec{\nabla}\theta \cdot \vec{\rho} \cdot \vec{\nabla}\theta$. Here we just consider (3.6) as fluctuations in the order-parameter space and calculate its probability of occurrence. See J. Langer and M. Fisher, Phys. Rev. Lett. 19, 560 (1967).

[11]M. C. Cross, J. Low Temp. Phys. 21, 525 (1975).

[12]That coreless 4π vortices will be driven in motion in a constant superflow maintained by a chemical potential difference was first pointed out by P. W. Anderson and G. Toulouse, Phys. Rev. Lett. 38, 508 (1977).

[13]V. Ambegaokar, P. G. de Gennes, and D. Rainer, Phys. Rev. A 9, 2676 (1974).

[14]For a detailed discussion on quantization of circulation on container surfaces, see, N. D. Mermin, in *Sanibel Symposium on Quantum Fluids and Solids*, edited by S. B. Trickey, E. D. Adams, and J. W. Dufty (Plenum, New York, 1977).

[15]The surface circulation can be established by first cooling the normal ^{3}He in a rotating container down below T_c, followed by a gradual reduction of the rotation of the container, so that in the final state, the normal fluid and the container are at rest.

[16]P. G. de Gennes and D. Rainer, Phys. Lett. 46A, 429 (1974).

[17]W. F. Brinkman and M. C. Cross (unpublished).

[18]N is taken as an even integer. Generalizing to the case of odd N is trivial.

[19]To see such an instability, it is sufficient to consider the stability of an array of singular 2π vortices in a two dimensional ideal fluid contained in the upper x-y plane $(y > 0)$, with their singular cores located at $((2\pi/u)n, w)$, $n = 0, \pm 1, \pm 2, \ldots$. To calculate the velocity field $\vec{v}$, we can imagine in addition to this vortex array, there were "image" -2π vortices located at $((2\pi/u)n, -w)$, as if the fluid were infinite in extent. The velocity $\vec{v}$ is just the resultant of the velocities due to these two rows of vortices. It is zero for $y \gg w$ and is parallel to $\hat{x}$ with an average value $u\hat{x}$ at $y = 0$. It can be shown that the quantity v^2 is a decreasing function of w. The layer is therefore attracted towards the boundary $(y = 0)$. Also see Langer and Fisher in Ref. 10.

[20]The more general argument for collapse of superflow in an annulus or a torus is that since the order parameters around any contour embedded in the annulus form a trivial loop in P_3, it can be deformed into a constant (see Lectures given by N. D. Mermin at the International School of Low Temperature Physics, Erice, Italy, 1977) (unpublished). However, the physical meaning of such a deformation, namely, vortex nucleation, is made clear only when described in terms of $\vec{v}_s$ and $\hat{l}$.

[21]The process (4.1) is different from the one we discussed in Sec. III when $T \sim 0$, which involves a t-dependent width $w(t)$. The latter is the process we have in mind here.

[22]This is another illustration of statements (a) and (b). The path is suggested by the bulk unstable mode, which is a circularly polarized textural distortion of the form $\hat{l} = \hat{z} + \lambda(\hat{x}\cos k_0 z - \hat{y}\sin k_0 z) = R(R(\hat{z}, -k_0 z)\hat{y}, \lambda)\hat{z}$, $\lambda \ll 1$, where $k_0 = u(c_0 + \frac{1}{2}\rho_s^{\parallel})/K_b$ is the critical wave vector in Ref. 3. It is easy to see that in the bulk region, $|x| \leq a$, the texture of (4.2) is circularly polarized when $t \ll 1$, though it does not have the critical wavelength. As for the latter, see the discussions in Ref. 3.

[23]See Volovik and Mineev in Ref. 7.